Journal of Evolving Space Activities
Vol. 1, Article No. 36, 2023
DOI: 10.57350/jesa.36

Development of Reusable Structures and Mechanisms for CALLISTO

By Sofia GIAGKOZOGLOU VINCENZINO,[1)] Silas EICHEL,[1)] Waldemar ROTÄRMEL,[1)] Felix KRZIWANIE,[1)] Ivaylo PETKOV,[1)] Etienne DUMONT,[2)] Anton SCHNEIDER,[2)] Silvio SCHRÖDER,[2)] Jens WINDELBERG,[3)] Tobias ECKER,[4)] and Moritz ERTL[4)]

[1)] *Institute of Structures and Design, DLR, Stuttgart, Germany*
[2)] *Institute of Space Systems, DLR, Bremen, Germany*
[3)] *Institute of Flight Systems, DLR, Braunschweig, Germany*
[4)] *Institute of Aerodynamics and Flow Technology, DLR, Göttingen, Germany*

(Received August 17th, 2022)

In the project CALLISTO (Cooperative Action Leading to Launcher Innovation in Stage Toss-back Operations) DLR, JAXA and CNES are jointly developing and building a demonstrator for a vertical take-off, vertical landing rocket first stage. CALLISTO aims to gather essential knowledge for the development of operational reusable rockets by demonstrating relevant technologies that are enabling recovery and reuse and leading to a sustainable launcher market. The development and design of reusable load-carrying structures is particularly challenging since the components have to withstand a variety of complex maneuvers for multiple times while keeping the maintenance and repair operations between flights to a minimum. This paper focuses on the progress of the design for CALLISTO's fairing, the deployable aerodynamic surfaces and the stowable approach & landing system considering the specific sizing load cases and functions during the mission. The challenges of movable structures, mechanisms and reusability are especially highlighted paying close attention on the detailed and individual design processes that are accompanied by analyses and pre-tests.

Key Words: CALLISTO, Reusable, Structures, Materials, Mechanisms

Nomenclature

AoA	:	Angle of Attack
ALS	:	Approach and Landing System
BLDC	:	Brushless Direct Current
CALLISTO	:	Cooperative Action Leading to Launcher Innovation for Stage Toss-back Operations
CFRP	:	Carbon Fiber Reinforced Polymers
CMC	:	Ceramic Matrix Composite
CNES	:	Centre National d'Études Spatiales
DLR	:	Deutsches Zentrum für Luft- und Raumfahrt e.V.
ESR	:	Equivalent Series Resistance
FEM	:	Finite Element Model
FCS/A	:	Flight Control System / Aerodynamic
FNS	:	Flight Neutralization System
GFRP	:	Glass Fiber Reinforced Plastic
GNSS	:	Global Navigation Satellite System
JAXA	:	Japan Aerospace eXploration Agency
LH2	:	Liquid Hydrogen
LLRM	:	Latch, Lock and Release Mechanism
LOX	:	Liquid OXygen
MRO	:	Maintenance and Repair Operations
NFM	:	Nose Fairing Module
PDR	:	Preliminary Design Review
RLV	:	Reusable Launch Vehicle
TPS	:	Thermal Protection System
VEB	:	Vehicle Equipment Bay

1. Introduction

The introduction of reusability in launch systems is expected to allow maintaining and even increasing the competitiveness of launch systems. In addition, reusability allows for a more sustainable space transportation. Starting from this analysis, JAXA, CNES and DLR decided to initiate the CALLISTO project as a cooperation in June 2017. The shared goal is to develop, build and fly a reusable scaled rocket stage taking-off and landing vertically.[1)] While the project is finishing phase B (Preliminary Design Reviews of the product (PDR-P) finishing) the first flight is planned from late 2024 from French Guiana. In total, CALLISTO will fly up to ten times. The two last flights called demonstration flights will be characterized by a flight domain and maneuvers relevant to an operational launch vehicle. CALLISTO will allow to gather unique technical and economic data which can be used to better evaluate whether Reusable Launch Vehicles (RLVs) make sense. CALLISTO will also allow to mature and master new technologies that will be useful for future launch vehicles.[2,3)]

In particular, in the case of structures and mechanisms, there is currently no experience in the space transportation sector in Europe. This know-how is now being built by DLR. It will be very useful for the development of future European reusable stages and launch vehicles. As a matter of fact, lessons learned from CALLISTO will be able to be applied directly. This will help to save time and money.

CALLISTO's goal of performing a flight profile that demonstrates critical maneuvers for a reusable first stage induces challenging conditions for the vehicle's structures and mechanisms.[4)] In addition to a classic ascent phase the demonstration flights include a powered tilt-over and boost back maneuver, an aerodynamically controlled descent while reaching the transonic region and a precise landing phase on a dedicated landing zone.[5] To allow the performance of this profile with minimal risk to the vehicle, an incremental test approach has been chosen that considers eight test flights in advance of the demonstration flights with increasing energy levels.[3,6] Fig. 1 illustrates the different flight types in relation to the energy range. Each type of flight will be performed twice. The envelope that reaches the highest energy range describes the demonstration flight profile.

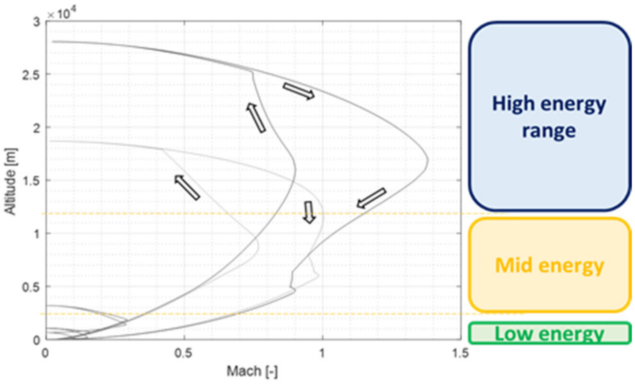

Fig. 1. Incremental increase of the flight envelope from low to high energy flights.

Based on this mission approach, structures and mechanisms have to withstand a variety of complex maneuvers for multiple times. An overview of the CALLISTO main structures is given in Fig. 2.

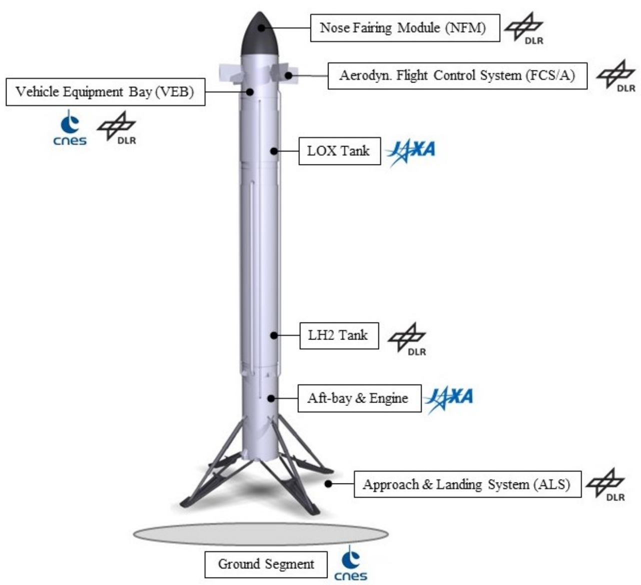

Fig. 2. CALLISTO main structures and responsibilities.

The components have to be studied in a very detailed way to reach an optimal performance during all flights and have to fulfil potentially opposing requirements to meet the needs of the different phases. The solution to this challenge can be found in the use of foldable and stowable structures. An active transformation of the vehicle's external shape by deploying certain components during specific flight phases allows individual reactions to different load cases while providing the functional aspects required for mission success. In the case of CALLISTO, this is achieved by deployable aerodynamic surfaces (fins) of the Aerodynamic Flight Control System (FCS/A) which fold out during the re-entry phase allowing the controllability of the vehicle, and stowable landing legs of the Approach and Landing System (ALS) which deploy shortly before touchdown allowing the vehicle to absorb the remaining kinetic energy and to stand autonomously on the landing platform.

The design process for deployable structures demands special attention due to the technical complexity and the limited experience in the field of reusability. The specific challenges of these structures and the experiences already gained are presented in this paper. In comparison, the example of the Nose Fairing Module (NFM) is described to represent the case of a solid structure without complex mechanisms, that is also heavily stressed due to the mission requirements. Main design difficulties identified at the PDR-Ps are described, reusability and Maintenance and Repair Operation (MRO) aspects are provided. In addition, DLR aerothermal numerical simulations, that serve as a basis for system requirement formulation and have a notable impact on the design process, are presented.

2. Nose Fairing Module

The primary function of the NFM is to protect the top of the CALLISTO demonstrator from aerodynamic flow, particularly necessary during the ascent flight phase. In addition, it accommodates the Global Navigation Satellite System (GNSS) antenna at the very top of the module and parts of the Flight Neutralization System (FNS) on the inner wall.

The NFM consists of three main sub-assemblies, which are depicted in Fig. 3.: The largest structure is the ogive main body. It is made from a CFRP sandwich with an aluminum L-flange bottom interface to the Vehicle Equipment Bay (VEB), an aluminum nose interface and a cork Thermal Protection System (TPS) on the outside. The CFRP sandwich is optimized to the mechanical loads driven by aerodynamic pressure on the outside and deformations due to aerodynamic forces onto the fins of the FCS/A. Therefore, not only the number of plies is locally decreased, but also the sandwich core is divided to implement a lighter core material on less stressed areas.

The separate nose sub-assembly is located on top of the ogive main body to accommodate the GNSS antenna and ensure best signal qualities. The whole nose sub-assembly is made from a radio frequency transparent material and is designed as a closed chamber to prevent condensation onto internal humidity-sensitive electrical components of the antenna. This is especially important for the descent phase, as the atmospheric pressure increase causes potentially humid air to enter into the inside compartments of the vehicle. The nose sub-assembly is equipped with one-way valves to reduce the pressure loads during the ascent. For the descent, the valves are

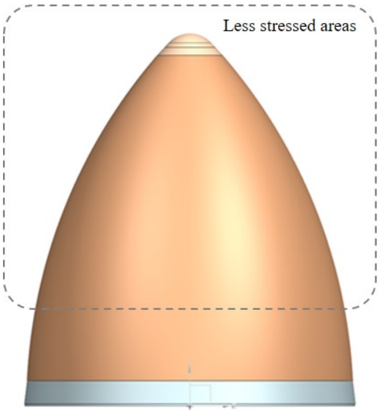

Fig. 3. Side view of the fairing module.

closed, so the resulting under pressure has to be withstood by the structure. However, this is more favorable than to withstand overpressure during ascent. The whole sub-assembly can be taken off in a sealed state in order to open and evaluate the status of the antenna in a controlled environment in-between the flights. An aerodynamic cover is added in four segments to the bottom interface over the L-flange to reduce drag.

One of the most critical loadings is the thermal environment. As the vehicle descends and the engine is restarted for a powered breaking maneuver, the vehicle is travelling through the hot engine exhaust plume. In order to quantify the external thermal environment a multitude of numerical simulations using the CFD solver DLR TAU,[7)] were performed for all applicable vehicle configurations (open fins / open and closed legs). For freestream conditions the appropriate atmosphere data for Guiana Space Centre is used. This is especially important for aerothermal aspects as the temperature of the oncoming air and the mixing with the hot exhaust gases play a key role in the prediction of the convective heat flux on the vehicle structure.

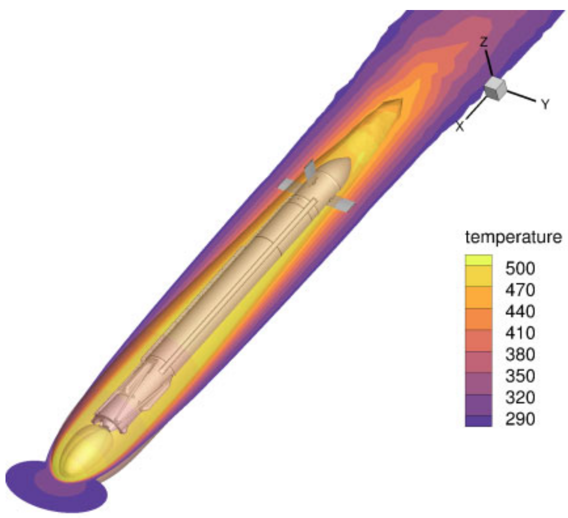

Fig. 4. CFD results for gas temperature [K] during boost phase (M=0.9837, 180° AoA). Plume for different mass fractions = 0.025, 0.1, 0.2 of exhaust gas is visualized as isosurfaces.

The gas temperatures around the vehicle at 180° Angle of Attack (AoA) for a point shortly after engine re-ignition are shown in Fig. 4. The oncoming air mixes with the hot engine exhaust gases and creates a plume around the vehicle. At high Mach numbers increased gas temperatures can be observed for most vehicle interfaces. Highest thermal loads for the demonstration flight are present after engine re-ignition at angles of attack between 180° and 170°. The thermal loads on the fairing at this point are shown in Fig. 5. for angles of attack 180° and 170°. The presence of the deployed fins is clearly visible in the heat flux distribution. High thermal loads are observable near the VEB interface, generally loads decrease towards the tip. When flying at an angle of attack of 170°, a larger share of the plume is redirected towards one side of the vehicle, leading to locally increased thermal loads.

Based on the thermal load distribution, the fairing surface is divided into five zones (compare Fig. 6). The zones are defined in cooperation between the designer and the aerothermodynamic experts and are important to achieve a more detailed temperature distribution for different regions as there are for example electronic components (GNSS antenna) implemented in the nose cone. There, a reliable temperature assessment is very important to ensure a proper functionality of the GNSS antenna. Mean and maximum values for these zones are extracted and assembled into an engineering database which allows interpolation for a given flight condition within the possible landing trajectory as a function of Mach number, density, angle of attack and configuration (open fins, open and closed legs). Based on this database, technical requirements for product design were derived at system level.

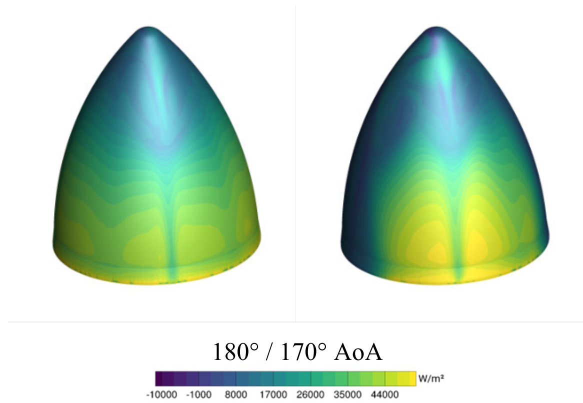

Fig. 5. CFD thermal loads at the beginning of the retro burn (M =0.9837).

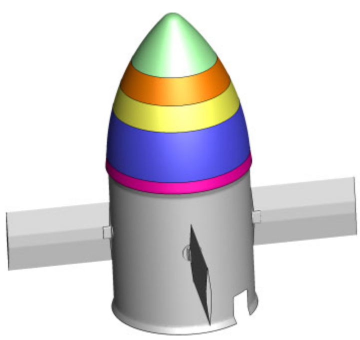

Fig. 6. CFD zoning fairing – VEB is displayed in grey for orientation.

The thermal environment is heating the structure to a point where chemical reactions in the cork TPS are about to start. One of the main challenges in assessing the reusability and determining the number of possible life cycles is to predict the material behavior of the cork in such a highly transient and turbulent environment. Therefore, sample tests are conducted to gain experimental data of the material behavior at that temperature domain. A hot air stream is directed onto the cork sample while varying the distance to the nozzle to replicate the streaming gas temperature over time. Especially the time is a crucial parameter, as it drives the progress of the chemical reactions within the material. The tests have shown that the irreversible reactions of the material are neglectable, since no ablation occurred. With regards to thermal conditions, the fairing is thus reusable for several flights.

Another challenge is the connection of the CFRP ogive main body and the aluminum L-flange, as the materials have very different thermal expansion coefficients. This could lead to a deformation of the structure, if the connection is not well-matched. For the CFRP, this parameter has to be considered in dependency of the fiber orientations to limit the reaction forces due to the thermal expansion.

The MRO aspects are driven by the fact that the fairing contains pyrotechnical equipment, which is part of the FNS. Special safety means are required to ensure a safe handling. The pyrotechnics, consisting of a pyrocord and detonators, are not only to be attached in a secure way, but also demountable, as they might be removed for MRO operations in between the flights. An attachment concept with a dedicated GFRP clip design is currently under investigation.

3. Aerodynamic Flight Control System

The purpose of the FCS/A is to ensure aerodynamic stability and controllability of the CALLISTO vehicle during descent flight while producing minimal aerodynamic drag during ascent. As shown in Fig. 7 the design consists of four deployable aerodynamic surfaces (fins) protruding from the VEB, each having a dedicated electromechanical actuator system with a deployment hinge mechanism and a Latch Lock and Release Mechanism (LLRM) interface with the LOX tank to be able to provide two different flight configurations for ascent and descent phase.

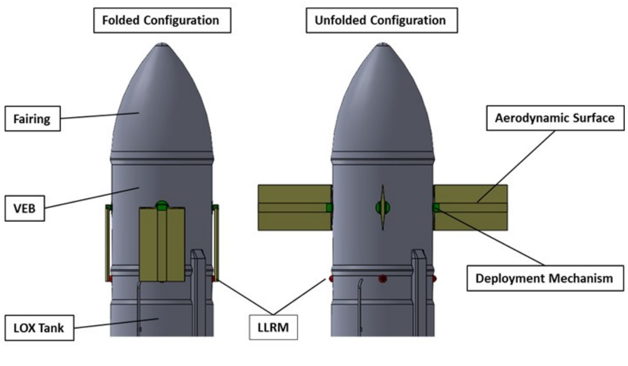

Fig. 7. FCS/A in ascent (left) and descent (right) configuration.

The FCS/A main actuator is a combination of highly dynamic compact servo motor, high precision encoders, high gear ratio harmonic drive (gearbox) and high load capacity bearings providing the necessary torque for holding and positioning of the aerodynamic surfaces. The central hollow shaft of the main actuator houses additionally a linear unfolding actuator which in turn consists of a high-speed low torque BLDC motor, a high gear ratio planetary gearbox and a roller screw spindle. To provide power and data link to the BLDC motor and sensors in the fin, a flexible cable is used. The main components are shown on the top of Fig. 8.

The secure holding of the fin in the folded configuration during the ascent flight phase of the vehicle and the separation at the beginning of the fin unfolding sequence is enabled by the LLRM which interfaces the fin and the LOX tank upper skirt.

The FCS/A deployment hinge mechanism is designed as a compact interface mechanism that enables the fin deployment and the transmission of the aerodynamic fin loads to the output shaft of the main actuator. It consists of a fin flange and a fin root having a guided sliding wedge of matching taper. The kinematic operation of the hinge is as follows: After initiating the fin unfolding sequence and the release of the LLRM, the fin root is pulled by the unfolding linear actuator. The wedge mechanism, with its guiding and sliding features, is designed in a way that the pulling/pushing motion translates to a rotation of the fin around an axis at the end of the pulling rod and simultaneously a linear motion enabling the wedge setting. By reaching the unfolded position the fin wedge joint is retained by friction. Partially this is done by the wedge taper itself. However, most of the hold down is accomplished by the pulling rod acting together with the gear of the actuator. It utilizes the ability of a high reduction ratio gear to be a very effective friction device when the direction of transmission is reversed (input shaft vs. output shaft). In addition to the powerless hold down capability, the mechanism is constantly being monitored by the hall sensors of the motor in a closed loop system. The unfolding sequence with the corresponding travel of the roller screw is shown in Fig. 8 for unfolding angle of a) 90°, b) 45° and c) 0°. Once the fins are in a perpendicular position (see Fig. 8c), a second rotation performed by the main actuator is started to reach final descent configuration that is shown in Fig. 7 and to be able to control each fin individually.

The high requirements on the FCS/A call for perfect interaction between fin, unfolding mechanism, motors, gears, sensors and controller. For each component within the FCS/A product load cases that are used for sizing vary significantly. Of particular importance is, for example, the torque that has to be generated by the motor in conjunction with gear ratio and drivetrain inertias (for more details see Ref. 8)), the aerodynamic and thermal loads for the fin, the deployment induced shock response of the LLRM and many others. But also, when it comes down to design details like the harness to connect the sensors in the fins, the requirements originating from reusability become apparent. Due to the unfolding kinematics, the harness (see right hand side of Fig. 8) has to undergo a 90° twist motion to reach a neutral fin position and is than subject to smaller twisting actions in the range of +- 20° according to the fin deflection necessary for a controlled flight.

These continuous motions lead to low cycle fatigue of the wires. A typical failure can be seen in Fig. 9 where the wire is broken at the crimped connector pin.

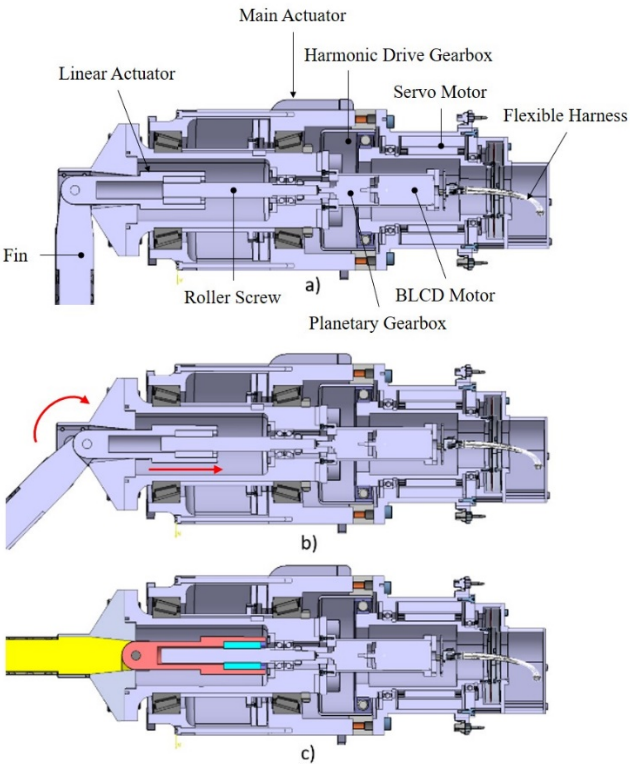

Fig. 8. Unfolding sequence induced by the linear actuator.

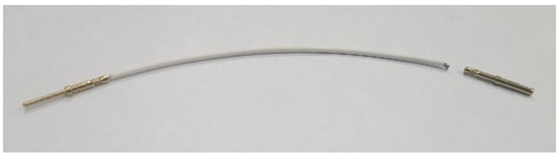

Fig. 9. Wire with low cycle fatigue failure.

The lifetime of this flexible harness has been tested in accelerated life time tests on a dedicated test rig where it was subjected to motion profiles expected to be present during flight. Five different wire configurations were tested to determine the most suitable one for the application. The test rig and set-up for the flexible harness is shown in Fig. 10.

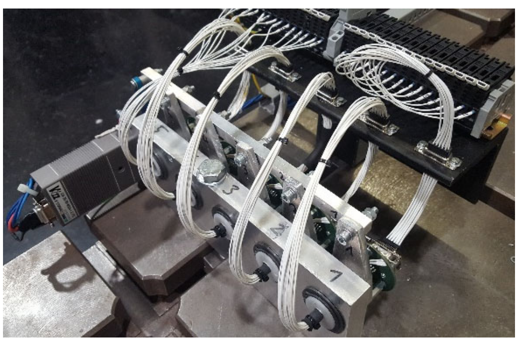

Fig. 10. Test rig for flexible harness.

As per now results from the preliminary lifetime tests indicate that the flexible part of the harness should be exchanged after each flight to reduce the probability of a low cycle fatigue failure. This of course has a significant impact on the MRO operations because the harness cannot be accessed while the actuator is installed in the VEB. To ease the installation and removal process as well as to shorten the therefore needed time, the actuator VEB interface was designed with this in mind. It consists of only eight bolted connections and assures proper electrical connection by self-aligning connectors that are engaged during the bolt fastening process for which no access to the internals of the vehicle is needed. In industrial applications transmission of electrical signals and power is typically done by slip ring connectors. For the needed dimensions no COTs slip ring could have been identified that would also withstand the vibrational environment, resulting in an expensive new development in conjunction with a dedicated qualification campaign.

All actuators and LLRMs are operated by a modular actuator controller box that consists of four identical fin actuator control electronics, four unfolding actuator control electronics, and a shared internal power supply featuring a buck boost converter, two large capacitors and a break resistor. A sectional view of the FCS/A controller can be seen in Fig. 11. To allow the communication with the vehicle network an Ethernet to CAN gateway is used. The internal power supply is used to convert

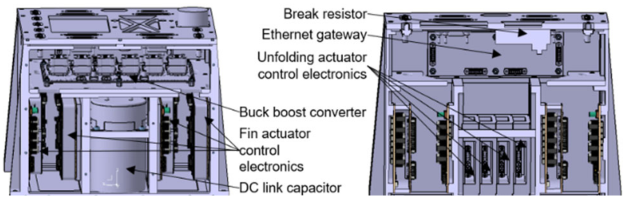

Fig. 11 Sectional views of the FCS/A controller.

the 28 VDC board net to 48 VDC and allow for an internal power management that can deal with short transient high power demand while the input power remains limited.

Due to the high frequency switching of high voltages and currents, EMC is a major concern for the power supply board and the actuator controllers. However, first prototype tests have shown the compliance to the EMC requirements of CALLISTO. Furthermore, the robustness of the large electrolytic capacitors against rapid de- and repressurization has been tested in a vacuum chamber. In this setup a batch of capacitors has been cycled between maximum and minimum expected pressure of the most demanding flight profile for a life cycle well beyond the envisaged ten flights. After each cycle the capacitors are checked for physical changes and their capacity and Equivalent Series Resistance (ESR) is measured. No degradation or failure could be identified in this campaign.

Additionally, hardware tests have already been performed on structural sub-component level and showed good results with regard to the requirements. Currently, functional test of the hinge mechanism and vibration tests of the LLRM are detailed as they are sizing for the adjacent vehicle structure. In parallel extensive Finite Element Model (FEM) analyses have supported the confidence in the developed design. Mechanical and thermal analysis of the structural components, as well as transient thermal simulations of the full controller under load have been performed and used for optimization.

Overall, the FCS/A design is driven by the reusability mission objectives. It is crucial that this complex electromechanical assembly can withstand the multiple load cycles envisaged. In order to minimize the occurrence of fatal malfunction and thus a mission loss, MRO procedure is also being carefully elaborated. It consists of preventive maintenance tasks after each flight, such as disassembly of the four FCS/A units, cleaning and inspection of their electromechanical components, exchange of the flexible harnesses, re-setting of the LLRMs, re-qualification of the actuators and potential repairs. Covering these points, the development of the FCS/A has successfully passed PDR.

4. Approach and Landing System

The ALS is the support system allowing the vehicle to stand autonomously without ground support equipment. During touchdown this system (1) absorbs the residual kinetic energy, (2) provides dynamic and static stability, (3) maintains the ground clearance limits and (4) limits the loads that transit to the rest of the vehicle. Ultimately, the ALS shall enable a safe transition from flight to ground state. The ALS landing legs are folded and locked against the vehicle body during ascent and descent and are deployed by the means of a pneumatic deployment subsystem shortly before touchdown. The deployment sequence starts with the opening of the solenoid valve, which allows the working gas to flow from the high pressure CFRP vessel into the primary strut assembly. Shortly after, the hold-down and release mechanisms are released. A spring driven push-off mechanism provides the torque required to drive the ALS landing leg assembly into a position, where the pneumatic drive becomes effective. This sequence is initiated by a signal from the on-board computer, which is turned into electrical power by the ALS Controller. After full extension, two latching mechanisms, which are located at the segment interfaces of the telescopic strut assembly, prevent the retraction due to external loading. The legs remain latched and locked until retrieval by ground segment.

The landing leg structural assembly consists of the primary and secondary structure shown in Fig. 12. The primary structure is the already mentioned telescopic structure assembled from four CFRP segments (segment 1, 2, 3a and 3b) connected by attached titanium flanges to the latching mechanisms (between segments 1-2 and segments 2-3) and the damping system (between segment 3a and 3b). For simple and precise deployment and to reduce wear and friction, segments 2, 3a and 3b are coated on the outer surface. Different variations of surface finish have been investigated leading to a diamond-like carbon coating on the outer surface of segment 2 and a polytetrafluoroethylene-based coating on segments 3a and 3b. Due to geometric boundary conditions, the coating could not be applied on the inner surfaces of segments 2 and 3a. For this reason, investigation of the uncoated CFRP surface is also necessary. Thus, coating efficiency and surface finish is an important aspect of design and functionality that needs to be verified by tests.

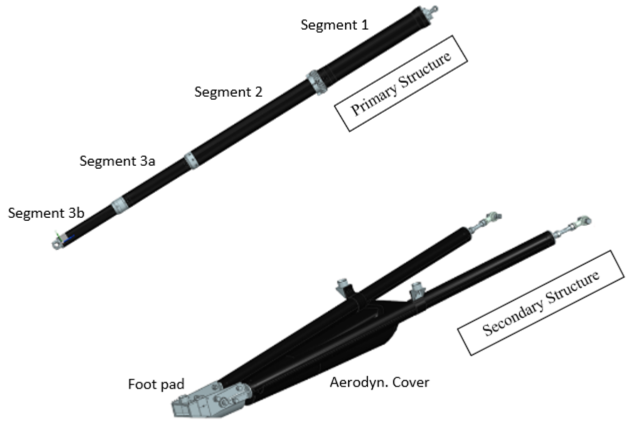

Fig. 12. ALS structure, primary structure (top) and secondary structure (bottom).

The primary structure is connected to the titanium foot pad and thus to the secondary structure by the lower connection element of segment 3b. The end dome of segment 1 provides the connection to the upper bracket of the CALLISTO aft-bay. The secondary structure consists of two main CFRP tubes bonded together by an aerodynamic CFRP cover. At the tapered end of this structure, the titanium foot pad is detachably mounted. At the opposite end, the titanium attachments are also detachably mounted to the CFRP tubes. The ball joints that are mounted on the titanium attachments provide the connection to the lower brackets of the CALLISTO aft-bay structure.

The foot pad includes a rubber layer on the ground facing surface that provides defined contact properties for landing on specific landing zones. The foot pad also has an integrated push-off mechanism to support the deployment.

Especially the latching and the extraction of the primary strut segments are critical for the reusability mission objectives, not only because an unsuccessful deployment will cause a mission loss, but because these processes affect the wear of the primary strut interfaces and latching mechanism. An extensive deployment test campaign has been conducted, in order to verify the preliminary design of the ALS and to assess the correlation of multiple landing leg deployments on the degradation of interfaces and structural design features, such as wear of coatings and latching mechanism parts. Fig. 13 shows the deployment test stand with a deployed landing leg. Due to time and cost constraints of this development model most of the struts were made from aluminum instead of CFRP. Only Segment 2 was made from CFRP as it is crucial for deployment and latching. This development model is used in thess first step to prove the functional chain and the kinematic constrains of the deployment sequence in a first test row. In a next step the aluminum parts will be replaced with flight realistic CFRP parts and the tests will be continued with focus on deployment characteristics. In addition, the measurements gathered during the deployment test campaign contributes to the validation of the numerical ALS deployment dynamics model, that is used for system level studies.[9]

As a result, it has been shown, that the primary strut segment interface design and tolerances are of crucial importance for the functionality and the purpose of re-usability. Too tight interface tolerances lead to higher segment to segment friction and hence have a negative effect on the unfolding capability and an increased wear of the sliding surfaces. On the other hand, wider tolerances enable an easier unfolding process but increase the clearance between primary strut segments, and hence reduce the load carrying capability at touchdown as a consequence of lower segment to segment interface stiffness.

Fig. 13. ALS landing leg development model in deployed state.

After deployment test campaign, parts of the latching mechanisms and of the primary strut assembly have been reused into the touchdown test campaign model, in order to imitate a complete life time of several ALS structural components. To test the damping behavior and the structural integrity of the landing leg, dedicated touchdown tests were performed. Fig. 14 shows the touchdown test stand.

Fig. 14. Side view of the touchdown test stand.

Beside those objectives, special focus was set on the reusability of the leg and its mechanisms.
After a first series of five touchdowns the leg was disassembled and all parts were checked. Main observations are listed below:

- The inner surface of segment 3a showed minor scratches in lateral direction, which is not critical, since it is in the direction of motion.
- The latching blocks of the latching mechanism showed almost no degradation.

Summarized from the experience gained through manufacturing and testing phase, the following points can be highlighted as particularly important for the primary and secondary structure at PDR-P:

- Handling of CFRP components of this size during the manufacturing process has a direct influence on the quality of the products. External punctual influences on the surfaces must be prevented.
- As large CFRP parts warp during the manufacturing process, these deformations must be considered for the final products.
- For surface coating, the geometrical data such as inner diameter and length is crucial. Small inner diameters and large lengths cannot be coated due to limitations in technical processing or can only be coated with great difficulty.
- For the coated struts the tolerances between the telescopic segments are one of the most critical aspects for the functionality of such a landing leg.

Further nondestructive testing is necessary to evaluate whole structural integrity of the material and interfaces to metallic parts. This also provides the opportunity to ensure the quality of the CFRP structure.

In addition to the mechanical challenges already described, for the ALS, critical heat loads arise during the retro propulsion phase of the demonstration flights. The engine is reignited to decelerate the descending vehicle. In this phase the hot exhaust gases from the engine are diverted onto the vehicle structure by the free stream flow as shown in Fig. 15 for a Mach number of 0.5 and an angle of attack of 170°.

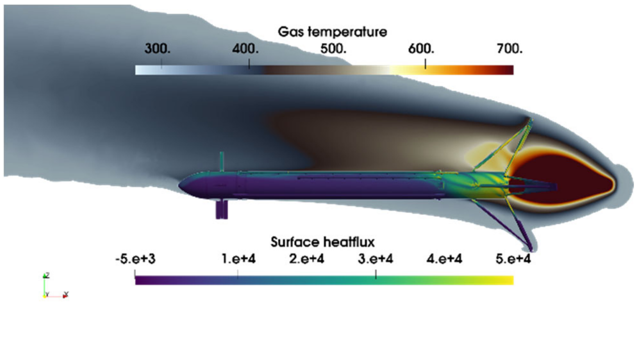

Fig. 15. Temperature field [K] and surface heat flux [W/m^2] for a configuration of CALLISTO with deployed landing legs at M=0.5, AoA=170°, engine thrust 100%, sideview.

An aerothermal database providing maximum and average heat flux predictions for different sections of the vehicle has been generated with steady state CFD simulations in order to help design for these loads. The simulations are done, using the DLR TAU code with the Spalart-Allmaras turbulence model. The database provides a parameter space of different flight Mach numbers, densities, angles of attack, angles of roll, leg deployment angles and thrust levels. All of these parameters influence whether a landing leg is inside the exhaust plume and thus heated, or not. This can be observed in Fig. 15, where the hot gases strongly interact with the landing leg on the upper side, while the lower landing leg is actually cooled by the free stream. The resulting heat fluxes are shown in Fig. 16 for the same parameters as for Fig. 15. Furthermore, it can be observed that certain zones, like the struts closer to the vehicle, are generally affected by the hot gases during retro propulsion.

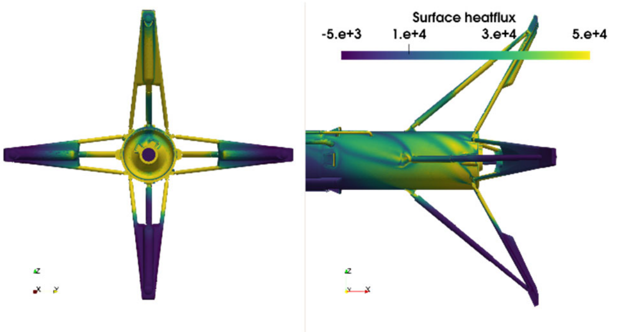

Fig. 16. Detailed heat flux [W/m^2] onto landing legs for M=0.5, AoA=170°. Left: bottom view, Right: sideview.

To consider these spatial differences in the aerothermal database the landing legs have been separated into smaller zones in post processing. Therefore, the secondary struts have been zoned as five radial segments with a top and bottom part each for ten total zones per strut, while the primary struts have been zoned as three radial segments. This zoning is especially important for an adequate design of the TPS. A specific thermal distribution by this zoning is needed for the estimation of the TPS thicknesses. The detailed dimensioning is important to safe mass for the whole vehicle. The zoning is visualized in Fig. 17.

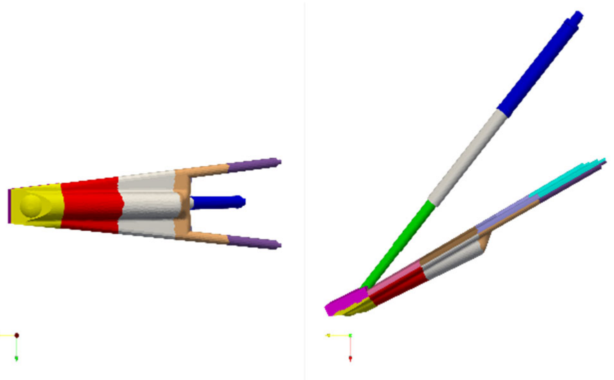

Fig. 17. Zoning of the landing leg for the aerothermal database.

In addition to the 3D CFD simulations for the flight 2D steady state simulations of the jet impingement on the ground have been done. These simulations vary height over ground and engine thrust level and provide the heat fluxes to determine the heating of the landing pad and thus the radiative environment post landing. Furthermore, the 2D simulations allow for identifying the height below which plume ground interaction affects the convective heat fluxes. This case has also been covered with an additional 3D simulation including a modelling of the ground.

The described calculations of critical heat loads are used as input for system analysis and result in requirements that indicates high thermal loading especially for the secondary structure of the ALS. For the demonstration flights a cork-based TPS will be required for these components. Detailed design and refurbishment logic of the TPS is still in progress and needs to be finalized in the next project steps considering a refinement of the system requirements and mission boundaries.

However, analysis of the test flights showed that the thermal loads of the first low-energy test flights are even more challenging since the vehicle is launching from deployed legs. Based on this situation, an additional and detachable Clip-TPS is foreseen for the first test flights due to increased thermal loads in order to protect the secondary structure and the TPS that is designed for the demonstration flights. For the remaining test flights and in particular for the demonstration flights, the Clip- TPS will not be used. As shown in Fig. 18, this Clip-TPS consists of a fiber-ceramic hard shell around the secondary cover and will be supplemented with insulation (high temperature insulation wool). It is designed to limit to the maximum temperature of the secondary structure so that no degradation of the material begins. It will be mounted to the secondary structure via an auxiliary structural frame.

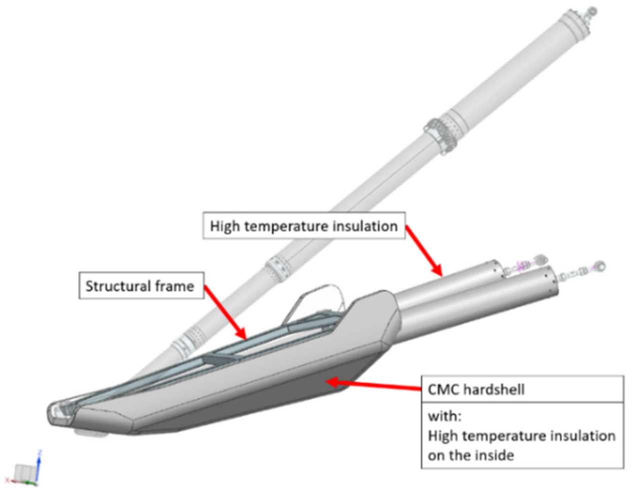

Fig. 18. Clip-TPS on landing legs for the first test flights of CALLISTO.

First manufacturing processes started on 1:5 scale shell. The experience on this model will be used to manufacture the original Clip-TPS shell. Besides the availability of the oxide fibers, the following points are interesting and important for the manufacturing and the use:

- The placement of the individual fabrics at theses curvature radiuses and overall size is challenging.
- There is limited experience in the handling of such a large and thin oxide Ceramic Matrix Composite (CMC) structure.
- The attachment of such a shell structure to the supporting structure needs further investigation.

5. Conclusion

The CALLISTO demonstrator faces most of the same challenges of an operational vertical take-off and vertical landing reusable rocket stage and thus deals with key aspects of RLVs. Deployable structures and reusable mechanisms are considered as a key technology and enabler to master the challenge of reusability. In the case of CALLISTO, good progresses have been achieved. Technical details are already advanced and well understood with the completion of the product PDRs. Preliminary test results and aerothermal calculations allow to solve detailed design issues and to prepare for the specific flight mission. Further extensive tests and qualification campaigns are required to achieve a flight ready vehicle and low mission risks. Extensive post flight analysis will be needed in order to understand all effects on material and structure with regard to reusability.

Acknowledgments

The authors would like to thank the entire CALLISTO project team at CNES, JAXA, and DLR for their remarkable efforts and collaboration over the past years.

References

1) Ishimoto, S., Tatiossian, P. and Dumont, E.: Overview of the CALLISTO Project, 32nd International Symposium on Space Technology and Science, Fukui, Japan, 2019-o-1-05, 2019, https://elib.dlr.de/132886/.
2) Dumont, E., Ishimoto, S., Tatiossian, P., Klevanski, J., Reiman, B. Ecker, T., Witte, L., Riehmer, J., Sagliano, M., Giagkozoglou Vincenzino, S., Petkov, I., Rotärmel, W., Schwarz, R., Seelbinder, D., Markgraf, M., Sommer, J., Pfau, D. and Martens, H.: CALLISTO: A Demonstrator for Reusable Launcher Key Technologies, *Trans. JSASS Aerospace Tech. Japan.,* **19** (2021), pp. 106-115, https://doi.org/10.2322/tastj.19.106.
3) Dumont, E., Ishimoto S., Illig M., Sagliano M., Solari M., Ecker T. et al.: CALLISTO: towards reusability of a rocket stage: current status, 33rd International Symposium on Space Technology and Science, Oita, Japan.
4) Giagkozoglou Vincenzino, S., Rotärmel, W., Petkov, I., Elsäßer, H., Dumont, E., Witte, L. and Schröder, S.: Reusable Structures for CALLISTO, 8th European Conference for Aeronautics and Space Science (EUCASS), Madrid, Spain, 2019, https://doi.org/10.13009/EUCASS2019-262.
5) Desmariaux, J., Cliquet Moreno, E., Chavagnac, C., Tatiossian, P. Saito, Y. and Dumont, E.: CALLISTO Reusable Vehicle System Design, 32nd International Symposium on Space Technology and Science, Fukui, Japan, 2019-g-02, 2019, https://elib.dlr.de/132889/.
6) Krummen, S., Desmariaux, J., Yasuhiro, S., Boldt, M., Briese, L., Cesco, N. Chavagnac, C., Cliquet Moreno, E., Dumont, E., Ecker, T., Eichel, S., Ertl, M., Giagkozoglou Vincenzino, S., Glaser, T., Grimm, C., Illig, M., Ishimoto, S., Klevanski, J., Lidon, N., Mierheim, O., Niccolai, J., Reershemius, S., Reimann, B., Riehmer, J., Sagliano, M., Scheufler, H., Schneider, A., Schröder, S., Schwarz, R., Seelbinder, D., Stief, M., Windelberg, J. and Woicke, S.: Towards a Reusable First Stage Demonstrator: CALLISTO - Technical Progresses & Challenges, 72nd International Astronautical Congress (IAC), Dubai, United Arab Emirates, IAC-21-D2.6.1, 2021, https://elib.dlr.de/147143/.
7) Schwamborn, D., Gerhold, T. and Heinrich, R.: The DLR TAU-code: Recent applications in research and industry. European Conference on Computational Fluid Dynamics (ECCOMAS CFD), Egmond aan Zee, The Netherlands, 2006.
8) Windelberg, J. and Maier, O.H.: Design of Flight Control Actuators for Reusable Launch Vehicles, Deutscher Luft- und Raumfahrt Kongress, 2021.
9) Schneider, A., Desmariaux, J, Klevanski, J., Schröder, S. and Witte, L.: Deployment dynamics analysis of CALLISTO's approach and landing system, *CEAS Space Journal (2021)*, 2021, https://doi.org/10.1007/s12567-021-00411-2.